

Section 4 Radio Astronomy

Chapter 1 Radio Astronomy.

Chapter 1. Radio Astronomy

Academic and Research Staff

Professor Bernard F. Burke, Professor David H. Staelin, John W. Barrett, Philip W. Rosenkranz, Michael Shao

Graduate Students

Ashraf Alkhairy, Tomas A. Arias, Pierino G. Bonanni, Christopher Carilli, Shiufun Cheung, Kevin Christian, Samuel R. Conner, Albin J. Gasiewski, Mark Griffith, Michael Heflin, Edward J. Kim, Charlene C. Kuo, Joseph Lehar, James C. Preisig, Jerome M. Shapiro, Howard R. Stuart, Bernard I. Szabo, Gregory W. Wornell

Undergraduate Students

Nicholas P.T. Bateman, Shiufun Cheung, Jee Chung, Stephen S. Eikenberry, Muriel Medard, Keith Tuson

1.1 Galactic and Extragalactic Research

Sponsor

National Science Foundation
(Grant AST 86-17172)

Project Staff

Professor Bernard F. Burke, Nicholas P.T. Bateman, Christopher Carilli, Jee Chung, Samuel R. Conner, Mark Griffith, Michael Heflin, Joseph Lehar, Keith Tuson

1.1.1 Gravitational Lens Search

An extensive search for examples of gravitationally lensed radio sources has been under way for several years, jointly with collaborators at Princeton and Caltech. The search begins with the material from the MIT Green Bank survey, carried out at Green Bank with a 300-foot telescope (now gone from the scene because of its collapse in November 1988). This survey was followed up by an extensive mapping program at the VLA. The result is the most extensive catalog of high resolution radio source maps in the world. We have established a data archive in RLE where our students and visitors can work with these materials. Of the 4000 sources that were mapped, 1000 have high

contrast, self-calibrated maps available. The preliminary reduction and first-order cleaned maps have been completed for the remaining 3000 sources. The full-self calibrated reductions should be completed during in the coming year.

The identification of gravitational lenses proceeds by examining the radio maps and identifying those sources whose multiple radio structure suggests the possibility of lensing. About ten percent of the sources meet the criteria. These sources are then studied optically, first in the continuum to see if there is optically visible structure, followed by spectroscopic observations to see which components have the same redshift. This procedure has allowed us to add six new objects to the list of known examples of lensing, which includes about sixteen cases in all.

Two especially interesting examples are shown in figure 1. The source MG1131 + 0456, (on the left, an example of an Einstein ring, the first found) described in last year's RLE report, has now been joined by a second example of an Einstein ring, MG1645+1346, shown on the right. In both instances, there is a foreground galaxy, with a background radio component so nearly aligned with the line of sight that a radio ring is generated by the action of the gravitational field of the galaxy and acts as a lens.

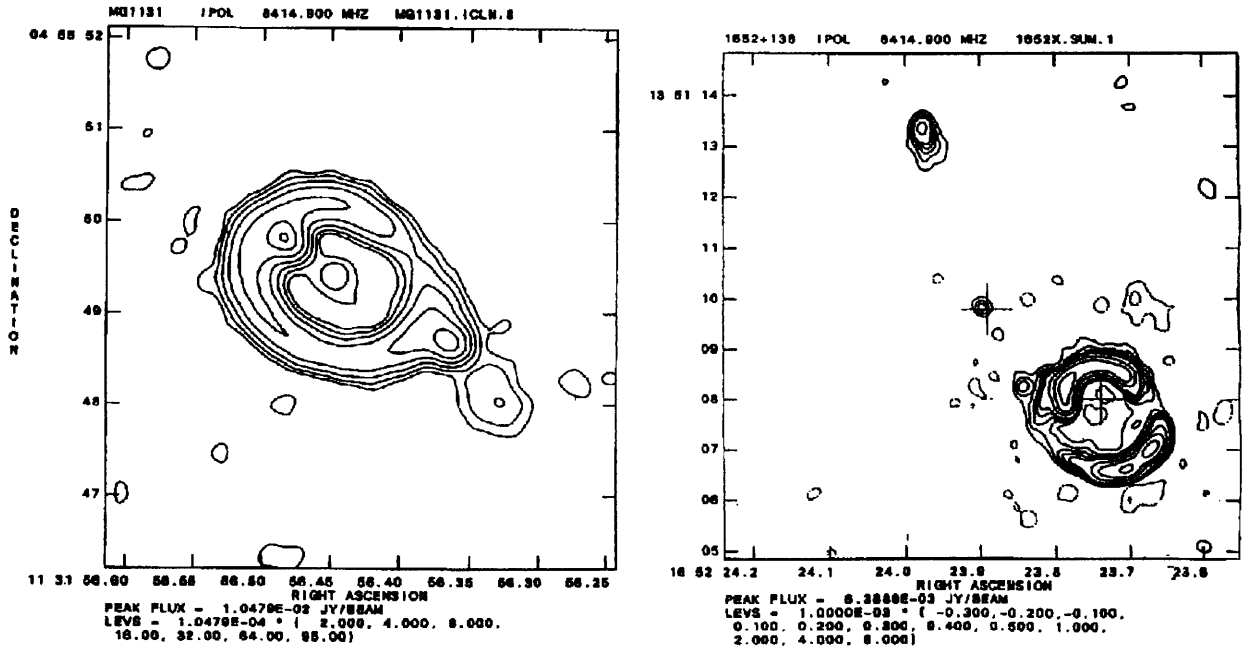


Figure 1.

1.1.2 VLBI Studies

The radio source 2016+112 is an example of a gravitationally lensed quasar, discovered by our group some time ago. The milliarc-second structure is now being studied with a view to explaining the detailed properties of the lens. The first generation of experiments is now complete; the preliminary maps were presented at the Boston meeting of the American Astronomical Society. There are curious anomalies present that require further observations. These have been scheduled for a world-wide VLBI session, using all the large radio telescopes in the world-wide net, which will be held in November 1989.

1.1.3 Time Variation of Gravitationally Lensed Quasars

The original double quasar, 0957+561, is an example of gravitational lensing that we have been monitoring for the past nine years. Most quasars fluctuate in brightness, and, if split into multiple images, the time variations

will show a lag in time that can be used to determine the Hubble constant in an entirely new way. The two main images of this quasar, which we observed with the VLA at 6 cm throughout the time frame from 1980 to 1988, show the expected variation, with the southernmost image (B) lagging the northern image (A) by 500 ± 100 days. This gives an estimate of $H_0 = 65$ km/sec/mpc for the Hubble constant, a value that is derived from a completely different data base compared to the conventional methods.

1.2 Orbiting VLBI

Sponsors

National Aeronautics and Space Administration
Jet Propulsion Laboratory

Project Staff

Professor Bernard F. Burke, Samuel R. Conner, Michael Heflin

1.2.1 QUASAT

The QUASAT VLBI satellite studies have now been completed. Neither the United States nor ESA has the resources to launch this kind of a satellite in the time frame of 1990 to 1995, while both the Soviet Union and Japan have separately decided to undertake similar missions. Professor Burke is chairman of a NASA working group to define and expedite the United States' cooperation in these missions which are known as RADIOASTRON and VSOP, respectively.

1.2.2 TDRSS Demonstration

In last year's *Progress Report*, we reported that a successful demonstration with the TDRSS satellite of the Orbiting VLBI principle had been carried out. Our group participated in the experiment under the leadership of G. Levy of the Jet Propulsion Laboratory. During the past year, the RLE Radio Astronomy Group built 15 GHz low noise amplifiers that were used by NASA and ISAS (the Japanese space agency) to perform a high frequency version, at Ku band, of the earlier TDRSS demonstration. From these tests, the feasibility of orbiting VLBI has been completely established.

1.3 High-Resolution Passive Microwave Imaging of Atmospheric Structure

Sponsor

NASA/Goddard Space Flight Center
(Grant NAG5-10)

Project Staff

Professor David H. Staelin, John W. Barrett, Pierino G. Bonanni, Albin J. Gasiewski, Philip W. Rosenkranz

A theoretical and experimental investigation of atmospheric sounding techniques using passive microwave observations near the

118-GHz (1^{-})O₂ resonance was largely completed.¹

This work involved model calculations, microwave observations of clear air and storms by an imaging microwave spectrometer on the NASA ER-2 high-altitude aircraft, and comparisons of theory with experiment.

A tropospheric and stratospheric planar-stratified radiative transfer model for millimeter wavelength radiation was developed. The gaseous absorbers are O₂ and H₂O, and the absorption and scattering by precipitation was modeled by sparse distributions of Mie spheres, assuming Marshall-Palmer liquid and Siskon-Srivastava ice size distributions with Henyey-Greenstein phase functions. A novel iterative method for computing the temperature weighting function for absorbing and scattering precipitation was developed.

These model calculations were compared with passive high spatial resolution (~1.5-km spot size) 118-GHz multichannel imagery of clear air and precipitation, as observed by the Millimeter-wavelength Temperature Sounder (MTS) instrument for 35 flights on the NASA ER-2 high-altitude aircraft during the GALE and COHMEX missions in 1986. The MTS is a double-sideband 8-channel 118-GHz scanning spectrometer with a 53.65-GHz single-beam radiometer. These comparisons between theory and experiment showed systematic differences in nadir brightness temperatures and scan curvature. The calculations were based on coincident radiosonde observations and used the Rosenkranz overlapping O₂ absorption line model. The cause of the discrepancies could not be unambiguously determined to be either experimental or spectroscopic. However, the discrepancies are consistent with an anomalous increase of ~15 percent in the 1^{-} line strength at altitudes near the tropopause.

Retrieval of precipitation cell-top altitude from the MTS 118-GHz data was demonstrated using a nonlinear statistical operator. The operator combines a Karhunen-Loeve

¹ A.J. Gasiewski, *Atmospheric Temperature Sounding and Precipitation Cell Parameter Estimation Using Passive 118-GHz O₂ Observations*. Ph.D. diss., Dept. of Electr. Eng. and Comp. Sci., MIT, 1988.

decomposition with rank reduction, linearization, and linear minimum mean-square-error estimation. The rms retrieval accuracy was 1.5 km for cumulus cell cores with top altitudes between 1.5 and 16 km. Decomposition of the MTS precipitation cell perturbation spectra reveals 2 to 3 observable degrees of freedom.

1.4 Tiros-N Satellite Microwave Sounder

Sponsor

SM Systems and Research, Inc.

Project Staff

Professor David H. Staelin, Charlene C. Kuo, Philip W. Rosenkranz

Present operational passive microwave spectrometers used on polar orbiting weather satellites will be superseded in the early 1990s by the Advanced Microwave Sounding Unit (AMSU). AMSU has 15 channels that simultaneously image the earth with 50-km resolution at frequencies distributed from 90 to 183 GHz.

This effort involves scientific support of the AMSU program with emphasis on atmospheric transmittance spectra and retrieval methods.

Much of the work is related to a statistical iterative scheme for estimating atmospheric relative humidity profiles for microwave radiometric measurements. The technique² overcame the nonlinearity and singularities intrinsic to this estimation problem. Simu-

lations showed that this new method yields rms errors in relative humidity estimates which are as much as 17 percent, 30 percent, and 40 percent lower than errors obtained using traditional linear statistical methods for polar, mid-latitude, and tropical climates, respectively.

Progress was also made in the development of methods for estimating precipitation parameters and surface emissivity. Development of concepts for passive microwave geosynchronous sounders also continued.

Concepts developed for the sounding of stratospheric and mesospheric temperature profiles using observations of the Zeeman-split oxygen lines were extended.³ A proposal for addition of such an instrument to the operational AMSU satellite instrument on the EOS satellite system was prepared and submitted to NASA.

1.5 Long-Baseline Astrometric Interferometer

Sponsor

U.S. Navy Office of Naval Research
(Contract N00014-86-C-2114)

Project Staff

Professor David H. Staelin, John W. Barrett, Edward J. Kim, Michael Shao, Howard R. Stuart

During 1988, development of the Mark III optical astrometric interferometer⁴ continued at the Mount Wilson Observatory, and additional scientific results were obtained.⁵ Oper-

² C.C. Kuo, *Statistical Iterative Scheme for Estimating Atmospheric Relative Humidity Profiles from Microwave Radiometric Measurements*. S.M. thesis, Dept. of Electr. Eng. and Comp. Sci., MIT, 1988.

³ P.W. Rosenkranz and D.H. Staelin, "Polarized Thermal Microwave Emission from Oxygen in the Mesosphere," *Radio Sci.* 23:721 (1988).

⁴ M. Shao, M.M. Colavita, B.E. Hines, D.H. Staelin, D.J. Hutter, K.J. Johnston, D. Mozurkewich, R.S. Simon, J.L. Hershey, J.A. Hughes, and G.H. Kaplan, "The Mark III Stellar Interferometer," *Astron. Astrophys.* 193:357 (1988).

⁵ M. Shao, M.M. Colavita, B.E. Hines, D.H. Staelin, D.J. Hutter, K.J. Johnston, D. Mozurkewich, R.S. Simon, J.L. Hershey, J.A. Hughes, and G.H. Kaplan, "Initial Stellar Diameter Measurements with the Mark III Interferometer," *Astrophys. J.* 327:905 (1988); D. Mozurkewich, D.J. Hutter, K.J. Johnston, R.S. Simon, M. Shao, M.M. Colavita, D.H. Staelin, B. Hines, J.L. Hershey, J.A. Hughes, and G.H. Kaplan, "Preliminary Measurements of Star Positions with the Mark III Stellar Interferometer," *Astron. J.* 95:1269 (1988); M. Shao, M.M. Colavita, J.L. Hershey, G.H.

ation of the interferometer in a photon-starved non-tracking mode was explored.⁶ A system was developed using a dispersive prism which projects the spectrum across the face of the same photon camera used for star-tracking. The relative flicker rates were measured for different optical spectral bands and the fringe visibility and fringe phase were estimated.

A real-time hardware engine computed and accumulated the autocorrelation of the detected spectrum from each coherent integration interval; a small computer determined the Fourier transform of these functions, and this transform was used to estimate the group delay. Tests using an internal white light source demonstrated that the usable path length difference was limited by the spectral resolution and detector artifacts to values between 14 and 26 microns. The detectability limit (SNR ~ 1) was found to be between 2 and 4 detected photons per 4-msec frame for tests using only 4000 frames (16-sec total integration time).

Because the present active fringe tracker cannot track at fluxes below 40 photons per 4-msec period, it appears that the magnitude limit for the Mark III interferometer can be extended by a factor of 10–20 (2.5–3.2 magnitude) for 16-sec integration. These results suggest that it should be possible to extend the detectability limit to $m_v \sim 13$ with one-meter apertures with separate processing within each r_0 subaperture and a total integration time of ~ 30 minutes. This system was used to track four bright stars. These are believed to be the first stellar observations of

dispersed-fringe group delay made with a visible-light stellar interferometer.

Work also began on an infrared detector to extend fringe position and visibility measurements to wavelengths of at least 1.1 microns, and perhaps 1.6 microns.

1.6 Video Image Processing

Sponsor

Center for Advanced Television Studies

Project Staff

Professor David H. Staelin, Shiufun Cheung, James C. Preisig, Jerome M. Shapiro, Bernard I. Szabo, Gregory W. Wornell

This effort has involved the publication of prior research results, and the continuation of work with motion estimation and image coding techniques. Optimal pre- and postfilters for multichannel signal processing were described in a recent paper,⁷ as were the results of work on optimal FIR pre- and postfilters for decimation and interpolation of random signals.⁸ Some image processing examples show that the mean-square optimal pair of filters leads to typical SNR improvements of 2–6 dB in comparison to other commonly used filter pairs.

A number of publications describing earlier work with the Lapped Orthogonal Transform (LOT) also were published. A paper on how a LOT can reduce “block” effects in image coding⁹ was followed by more complete

Kaplan, J.A. Hughes, D. Mozurkewich, D.J. Hutter, R.S. Simon, K.J. Johnston, E.J. Kim, and D.H. Staelin, “Wide-Angle Astrometry with the Mark III Stellar Interferometer,” *Bulletin of the American Astron. Soc.* 20:1005 (1988); abstract of paper presented at the 173rd Meeting of the American Astronomical Society, Boston, Massachusetts.

⁶ E.J. Kim, *Dispersed Fringe Group Delay Astrometry Using the Mark III Stellar Interferometer*. S.M. thesis, Dept. of Electr. Eng. and Comp. Sci., MIT, 1989; E.J. Kim, D.H. Staelin, M. Shao, and M.M. Colavita, “Dispersed Fringe Group Delay Astrometry with the Mark III Optical Interferometer,” *Bull. Amer. Astron. Soc.* 20:1006 (1988); abstract of paper presented at the 173rd Meeting of the American Astronomical Society, Boston, Massachusetts.

⁷ H.S. Malvar and D.H. Staelin, “Optimal Pre- and Postfilters for Multichannel Signal Processing,” *IEEE Trans. on Acoustics, Speech and Sig. Proc.* 36:287 (1988).

⁸ H.S. Malvar and D.H. Staelin, “Optimal FIR Pre- and Postfilters for Decimation and Interpolation of Random Signals,” *IEEE Trans. on Comm.* 36:67 (1988).

⁹ H.S. Malvar and D.H. Staelin, “Reduction of Blocking Effects in Image Coding with a Lapped Orthogonal Transform,” *Proc. ICASSP*, New York, April 11–14, 1988 (Paper M2.8).

papers on the same subject. One dealt with intraframe video coding experiments for 256 x 240 pixel images using 0.1–0.35 bits/pixel. The LOT was also used in interframe full-motion video coding experiments with head-and-shoulder sequences at 28 and 56 kbits/s.¹⁰ A subsequent paper described the LOT more completely and presented a fast algorithm for a nearly optimal LOT.¹¹ Unlike earlier approaches to the reduction of blocking effects, the LOT actually leads to slightly smaller signal reconstruction errors than does the DCT.

A paper on transform image coding with new families of models was also presented.¹² For example, a 2 dB improvement over the Chen and Smith scheme was obtained with a constrained coder with 128 classes operating at 0.5 bits/pixel; each coder was optimized for its own subclass of image. A sidechannel conveys information concerning which coder was employed.¹³ Another paper described a channel-compatible 6 MHz HDTV distribution system; this system is not compatible with NTSC.¹⁴

Work was also completed during the year on developing analytical foundations for pixel-based video displacement estimation.¹⁵ Convergence properties of local displacement estimation were examined, as were the accuracy of those estimates as a function of image brightness noise statistics. It was shown that local estimation followed by

regional estimation yielded performance that was relatively insensitive to the size of the region employed in local estimation.

1.7 Nonthermal Radio Emission from the Jovian Planets

Sponsors

NASA/Goddard Space Flight Center
(Grant NAG5-537)

Project Staff

Professor David H. Staelin, Tomas A. Arias,
Stephen S. Eikenberry

The Planetary Radio Astronomy (PRA) experiment on the Voyager 1 and 2 spacecraft observed radio emission from Earth, Jupiter, Saturn, and Uranus in 198 channels distributed over the band from 1.2 KHz to 40.5 MHz.

Earlier studies of Jovian decametric arcs and Alfvén currents were published.¹⁶ One study suggests that the Jovian Alfvén currents may be able to radiate at several different cone angles simultaneously, and that these Alfvén waves may survive for many hours at least. Analyses of striated spectral activity in Jovian and Saturnian radio emission, which is concentrated below 1 MHz, were also

¹⁰ P.M. Cassereau, D.H. Staelin, and G. de Jager, "Encoding of Images Based on a Lapped Orthogonal Transform," *IEEE Trans. on Comm.* 37:189 (1989).

¹¹ H.S. Malvar and D.H. Staelin, "The LOT: Transform Coding Without Blocking Effects," *IEEE Trans. Acoustics, Speech and Sig. Proc.* 37:553 (1989).

¹² G.W. Wornell and D.H. Staelin, "Transform Image Coding with a New Family of Models," *Proc. ICASSP*, New York, April 11-14, 1988 (Paper M2.7).

¹³ G.W. Wornell, *Transform Image Coding with Composite Block Source Models*. S.M. thesis, Dept. of Electr. Eng. and Comp. Sci., MIT, 1987.

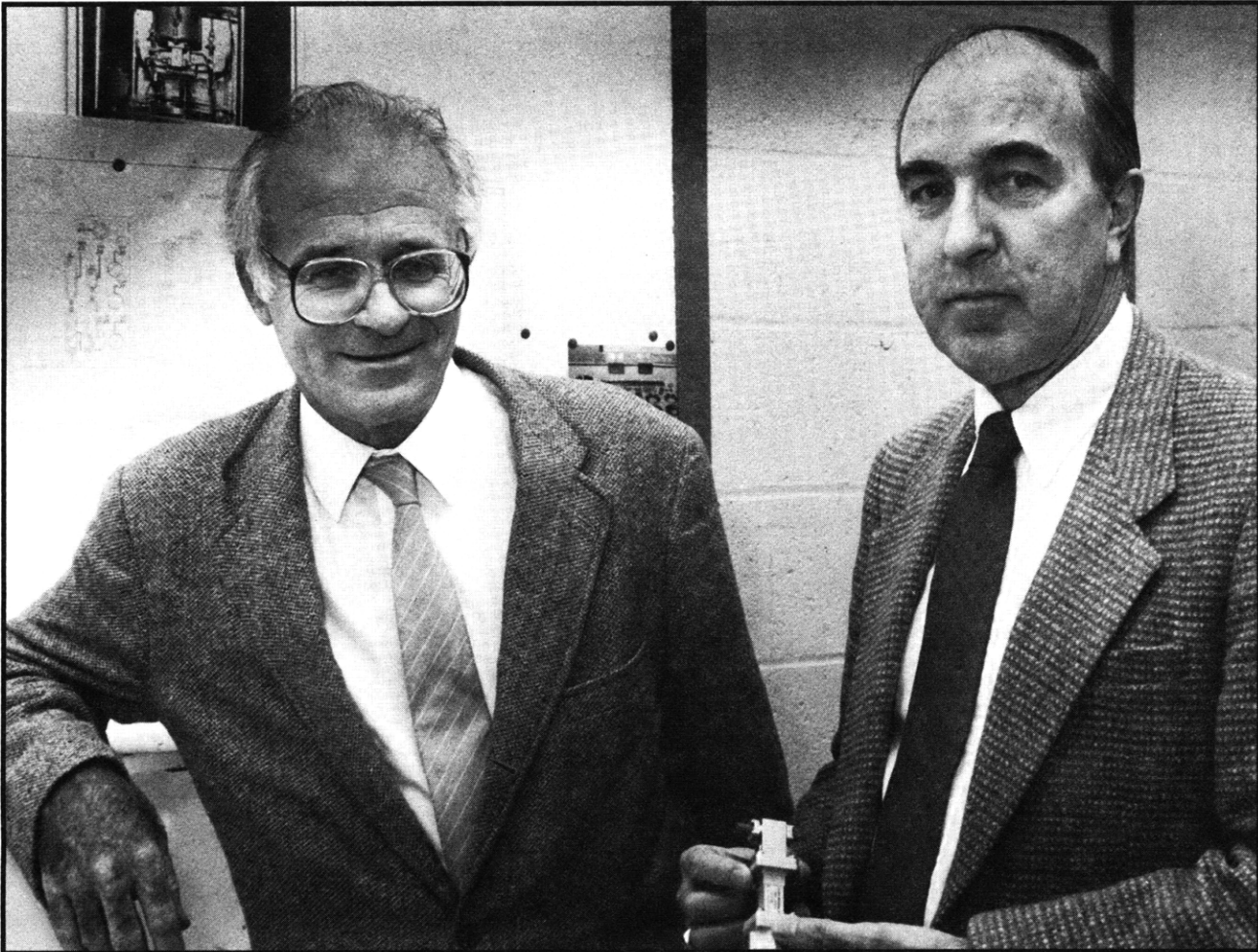
¹⁴ W.F. Schreiber, A.B. Lippman, A.N. Netravali, E.H. Adelson, and D.H. Staelin, "Channel-Compatible 6-MHz HDTV Distribution Systems," *SMPTE J.* 98:5 (1989).

¹⁵ B.I. Szabo, *Analytical Foundations of Pixel-based Video Displacement Estimation*. Ph.D. diss., Dept. of Electr. Eng. and Comp. Sci., MIT, 1988.

¹⁶ D.H. Staelin, P.M. Garnavich, and Y. Leblanc, "Jovian Decametric Arcs and Alfvén Currents," *J. Geophys. Res.* 93:3942 (1988).

published.¹⁷ Periodically this banded emission can vary on a time scale of seconds and can have an asymmetric dependence on frequency that is difficult to explain theoretically. In particular, plots of single 6-s frequency sweeps often exhibit a slow rise in intensity followed by a sharp drop off in each band as frequency decreases. New analytical

work emphasized development of improved representation of the spectral phenomenology of Uranian radio emission.¹⁸ The major observed categories of emission spectra for Uranus were defined and studied. Several of these categories resemble the striated spectral activity observed at Jupiter and Saturn.



Professor Bernard F. Burke (left) and Sponsored Research Technical Staff John W. Barrett

¹⁷ J.R. Thieman, J.K. Alexander, T.A. Arias, and D.H. Staelin, "Striated Spectral Activity in Jovian and Saturnian Radio Emission," *J. Geophys. Res.* 93:9597 (1988).

¹⁸ D.H. Staelin and S.S. Eikenberry, "Spectral Phenomenology of Uranian Radio Emission," *Bull. Amer. Astron. Soc.* 20:1089 (1988); abstract of paper presented at the 173rd Meeting of the American Astronomical Society, Boston, Massachusetts.

